GEOPHYSICS, VOL. 83, NO. 4 (JULY-AUGUST 2018); P. U43–U50, 9 FIGS.
10.1190/GEO2017-0569.1

Seismic velocity estimation using time-reversal focusing

Ariel Lellouch[1] and Evgeny Landa[1]

ABSTRACT

Seismic velocity estimation is a challenging task, especially when no initial model is present. In most cases, a traveltime tomography approach is used as a significant part of the workflow. However, it requires noise-sensitive, time-consuming picking and uses a ray approximation of the wave equation. Time reversal (TR) is a fundamental physical concept, based on the wave equation's invariance under TR operation. If the recorded wavefield is reversed and back-propagated into the medium, it will focus at its original source location regardless of the complexity of the medium. We use this property for seismic velocity analysis, formulated as an inversion problem with focusing at the known source location and onset time as the objective function. It is globally solved using competitive particle swarm optimization and an adequate model parameterization. This approach has the advantages of using the wave equation, being picking-free, handling low signal-to-noise ratio and requiring neither information on the source wavelet nor an initial velocity model. Although the method is discussed in the framework of direct source-receiver path acquisition, the foundations for its use with conventional reflection data are laid. We have determined the method's usefulness and limitations using synthetic and field crosshole acquisition examples. In both cases, inversion results are compared with a standard traveltime tomography approach and illustrate the advantages of using TR focusing.

INTRODUCTION

The subsurface seismic velocity field is usually estimated using traveltime tomography methods. Their first limitation is the necessity to pick arrival traveltimes, which induces errors and often requires manual intervention. In addition, because they rely on ray tracing for the calculation of source-receiver paths, they suffer from the high-frequency ray approximation, are unable to handle multi-arrival events, and practically require smooth velocity models for computational stability. Finally, they depend on local optimization methods in minimizing the difference between computed and measured traveltimes. Full-waveform inversion (FWI), on the other hand, uses the entire wavefield and inverts for subsurface properties. It is a highly nonlinear data-fitting procedure, which minimizes the misfit between recorded and modeled data. In its conventional form, the inverse problem is usually limited to low-frequency data and models, is solved by local optimization, and requires knowledge of the source wavelet (Virieux and Operto, 2009).

In this study, we suggest a new approach to velocity model estimation, based on the principle of the time-reversal mirror (TRM), proposed by Fink (1992). Instead of ray tracing and traveltime computation, it operates using the wave equation. Additionally, it does not require first-arrival picking nor prior information on the source wavelet.

Time reversal (TR) is a basic physical principle, consisting of time-reversing and back-propagating a recorded wavefield through the medium with the aim of refocusing it at its true source location (Figure 1). Symmetry of the wave equation under TR provides the intuitive justification for TR focusing at the original source location. A seismogram $\varphi(r_i, t)$ registered at locations $r_i (i = 1 \ldots N)$ is time reversed and emitted back as sources at the original receiver positions r_i. Regardless of the medium complexity, energy will, assuming the acquisition system is ideal, refocus at the original source location. This principle can be found in various applications: ultrasound and underwater acoustics, brain therapy, lithotripsy, nondestructive testing, and telecommunications (Fink, 1999). It is argued by Rose (2002) that TR combined with focusing analysis is a basis of exact inverse-scattering theory.

TRM is an extension of this principle to practical acquisition setups. In seismic applications, TR plays a major role in reverse time migration (RTM). In RTM (Baysal et al., 1983), the recorded wavefield is numerically back-propagated through an estimated subsurface velocity field. Because RTM involves solving the two-way wave equation, backward and forward propagations are applied

Manuscript received by the Editor 24 August 2017; revised manuscript received 20 March 2018; published ahead of production 23 April 2018; published online 25 June 2018.
[1]Tel Aviv University, Department of Earth Sciences, Tel Aviv, Israel. E-mail: lellouch@gmail.com; evgeny.landa64@gmail.com.

to the receiver and source wavefields, accordingly. For the latter, a priori, external knowledge of the source function is required, and its wrong estimation might lead to artifacts and smearing in the final image. Back propagation is followed by the application of an imaging condition, which is usually chosen as the zero-lag cross-correlation, or multiplication, of the source and receiver back-propagated wavefields. The product is subsequently stacked over all back-propagation times and source locations. This conventional imaging condition, alas, causes spurious events that arise from crosscorrelation between different nonreflective events (diving or head waves) and backscattered ones. This effect is most noticeable when sharp boundaries are present because they create strong coherent artifacts that mask the earth's reflectivity (Guitton et al., 2007; Díaz and Sava, 2016).

Motivated by the fundamental TR principle, we suggest a new method for seismic velocity analysis, extending earlier studies (Landa and Lellouch, 2017; Lellouch and Landa, 2017). Instead of conducting TR experimentally, we apply the back-propagation step numerically through an estimated velocity model. If this model is correct, the recorded wavefield will focus at its known source location and onset time after TR and back propagation. Because this focusing can be quantitatively measured, it is used as an objective function for an inversion problem. Similar concepts, using focusing as a criteria for velocity model correctness, have recently been introduced (Huang et al., 2017; Witten and Shragge, 2017). The former uses source-receiver extension, allowing the seismic source to depend on the source and receiver coordinates, and it subsequently measures the variance of the seismic source in the extended space to estimate the velocity model quality. The latter uses focusing between elastic mixed mode (PP, PS, SP, and SS) images in an extended image domain for velocity correctness estimation. TR was also recently suggested by Shustak and Landa (2017) to spatially localize subsurface sources for passive seismic and scatterers for active seismic. The proposed procedure consists of additional focusing analysis at each time slice (snapshot) because the onset time of a passive source or scattering point is unknown, but in that case, the velocity field was assumed to be correct.

The proposed velocity inversion approach is exemplified for direct-path (no reflections) acquisitions. It has several major advantages when compared with traveltime tomography, which is the natural choice for velocity model estimation in such scenarios. It does not require traveltime picking, handles low signal-to-noise ratio (S/N) data, and uses the wave equation for propagation. In addition, it is based on and commands the application of global optimization methods, which are independent of the chosen initial velocity model. Using synthetic and field crosshole examples, we illustrate the suggested workflow and compare it with conventional traveltime tomography, showing its usefulness.

TIME REVERSAL: BASIC PRINCIPLES

For simplicity, we consider an acoustic TR focusing case. Given the velocity $v(x,z)$ and density $\rho(x,z)$ fields, the wave equation of the pressure $p(x,t)$ is given by

$$\nabla\left(\frac{\nabla p}{\rho}\right)-\frac{1}{\rho v^2}\frac{\partial^2 p}{\partial t^2}=0. \tag{1}$$

Because this equation only contains a second-order time-derivative operator, it is invariant under TR. Therefore, if $p(x,t)$ is a solution, $p(x,-t)$ is also an acceptable one. It holds for an elastic equation as well (Van Manen et al., 2006). However, due to the noncausality of the $p(x,-t)$ solution, we limit ourselves to $p(x,T-t)$, where T is the overall recording time. It is assumed large enough so that $p(t>T)=0$.

From an experimental point of view (Fink, 1992), this requires sampling the entire volumetric field $p(x,t)$ in the interval $0\le t\le T$ and then retransmitting it in the whole volume as $p(x,T-t)$. This is, of course, unfeasible because it would require receivers in all subsurface points. Therefore, a more realistic approach is to take advantage of the Kirchhoff principle — given knowledge of the pressure and its normal derivative on any closed surface surrounding the volume, we can calculate the wavefield in any point in the volume. Therefore, a TR operation can be reduced to a 2D surface. Under this approach, the ideal experiment is such — a point source creates a spherical wavefront distorted by the inhomogeneous media in which it propagates. It is recorded on a closed surface along with its normal derivative. In the back-propagating step, we assume that on the enclosing surface, we are capable of creating secondary sources that correspond to the time-reversed pressure and its normal derivative. Under these assumptions, it can be shown (Cassereau et al., 1990; Fink, 1992; Anderson et al., 2008) that the time-reversed pressure field will be focused at the original source location. This property holds for any inhomogeneous medium, including cluttered media (Borcea et al., 2006). In fact, it has been shown that the more complex the medium is, the better focusing will be, even upon surpassing the Rayleigh resolution limit (Blomgren et al., 2002; Fink, 2006; Cao et al., 2012). This

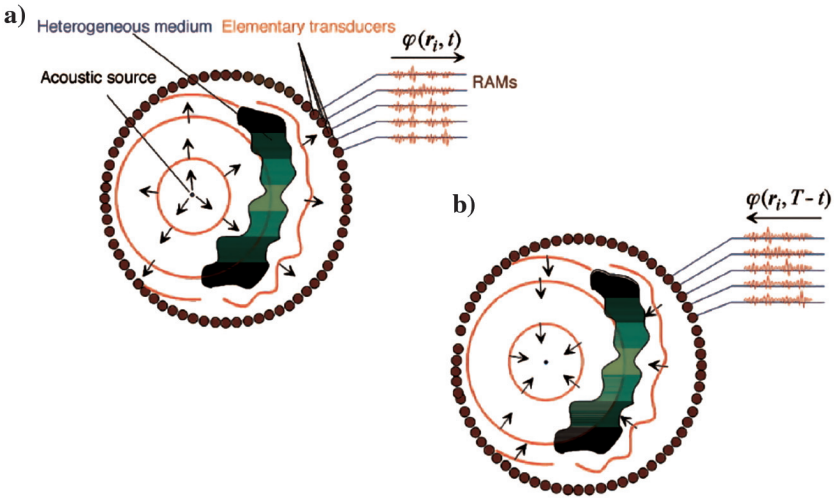

Figure 1. Illustration of the TR principle. (a) Recording step: A closed surface is covered with receivers. A point-like source generates a spherical wavefront that is distorted by medium heterogeneity. The distorted pressure field is recorded on the surface of the receivers. (b) TR step: recorded signals are time-reversed and reemitted at the position of the receivers. The time-reversed pressure field back-propagates and refocuses exactly on the initial source (modified from Fink, 2006).

property may be very beneficial when dealing with complex structures and limited acquisition setups.

In a realistic seismic acquisition scenario, we can no longer assume an enclosing surface upon which receivers are placed or a measure of the normal derivative of the recorded field. Instead, we will apply the same principle given the available acquisition, being aware of the fact that focusing will be imperfect and acquisition dependant (Cassereau and Fink, 1993; Bazargani and Snieder, 2016).

In addition, TR suffers from several inherent limitations in terms of source refocusing. First, complex wavenumbers, yielding evanescent waves, e.g., over critical reflections, cannot be recovered. Because they decay exponentially with distance from their origin, they will not always be recorded by the experimental setup (Anderson et al., 2008) and if so, cannot be refocused. However, Schuster et al. (2012) demonstrate that using TR and near-field seismic energy generated by scatterers in the vicinity of either source or receivers, superresolution can be achieved. Second, the acoustic or seismic signals have a finite bandwidth. Information encoded outside this bandwidth will be inevitably lost. Finally, this formulation is inaccurate for frequency-dependant dissipation, e.g., viscoelastic propagation. It is important to remember these limitations and their effects on the observed nonideal focusing.

TIME REVERSAL FOR VELOCITY ANALYSIS

We suggest computationally conducting TR for velocity model analysis. In this study, we limit ourselves to acquisitions in which direct paths connect sources and receivers, e.g., vertical seismic profiling (VSP), reverse VSP (RVSP), crosshole, and diving waves. Extension to reflected events will not be discussed here. In direct-path configurations, each source's location and onset time are known. Therefore, we can apply TR numerically using different trial velocity models. The one that focuses the recorded energy at its true position at time $t = 0$ is effectively the most correct velocity model.

Because the seismic data have a limited bandwidth, they will not focus to a Dirac delta function in time, but rather to a certain wavelet. We assume this wavelet is unknown, even though a priori information about it could be used as a correct focusing criterion. In addition, the acquisition geometry is rarely, if ever, surrounding the source. Therefore, focusing is expected to be of limited spatial resolution as well because we are effectively using an antenna of limited aperture for back propagation (Blomgren et al., 2002). Acquisition footprints might also be present in the spatial focusing pattern (Bazargani and Snieder, 2016). Finally, we have no practical way either of knowing the normal derivative of the pressure field or of imposing it as a boundary condition for the TR step, hence limiting ourselves to using the pressure field only.

Despite focusing imperfections, a stable measure of its quality is required. Because the spatial variation of the focusing is too geometry-dependant to be reliably used, we opt for a temporal-only criterion. At each known source point, we extract a part of the back-propagated trace. Because we know that focusing should occur at $t = 0$, the trace is extracted within a symmetric time window $[-T, T]$ around it, with T usually chosen as 20 ms. This implies using negative times, i.e., continuing back propagation after $t = 0$ is reached. As stated earlier, we do not want to assume knowledge of the source wavelet. Instead, assuming multiple sources in the survey, we expect all of them to have the same temporal behaviour. Because their absolute focused amplitude might differ due to coupling, source directivity, and receiver coverage, we normalize each focused trace by its absolute maximum value. In cases in which the radiation pattern has a strong effect on the data, especially polarity reversal, a more complex treatment than normalization is needed. Extracting the signal's envelope is the most straightforward solution (Witten and Shragge, 2017), but the signal resolution is decreased. Another option is to coarsely correct for the source mechanism, assuming it is known or can be estimated from the data. Since we are eventually interested in the kinematic pattern of the source and normalize each trace, such corrections may be conducted rather coarsely.

Subsequently, we measure coherency between focused sources within the time window around $t = 0$ using a minimum variation criterion. If TR focusing along the well is composed of traces $d_{i,t}$, assuming $i = 1 \ldots N$ when N is the number of sources, each containing the time interval $[-T, T]$, which consists of a total of W time samples around the true onset time ($t = 0$), the variation criterion E is calculated by

$$E = \sqrt{\frac{\sum_{i=1}^{N} \sum_{t=-T}^{T} \left(d_{i,t} - \frac{\sum_{j=1}^{N} d_{j,t}}{N} \right)^2}{N \cdot W}}, \tag{2}$$

which is, in fact, the average total difference, in the root-mean-square sense, between the back-propagated sources at their known locations and their average along the sources' dimension. This variation functional may be used as a basis for a global optimization scheme because it will be minimal when the velocity is correct and it will increase otherwise. In this study, we followed the competitive particle swarm optimization (CPSO) approach (Luu et al., 2016) to minimize E. In PSO, several simple entities, referred to as particles, are randomly positioned in the search space of some function and each one evaluates the objective function at its current location. Then, each particle determines its movement through the search space by combining its own current and best locations in the search space with the best location of the entire swarm, after applying some random perturbations. The next iteration takes place after all particles have been moved. Eventually, the swarm as a whole is likely to move close to an optimum of the objective function (Poli et al., 2007). The competitive part (CPSO) reinitializes particles that are close to one another (in the search-space sense) if their current objective function estimated value is not among the best in the swarm.

No initial model was supplied except for the upper and lower velocity boundaries. Inversion was conducted in two stages — first, an optimal 1D model was found. Then, it was used as a basis for a 2D model derivation, assuming a certain maximum deviation from the optimal 1D (usually 20%). As for any global optimization procedure, the computational costs are much higher than in conventional tomography, especially because we use the more computationally demanding wave equation. The number of receivers does not affect computation time because all receivers of a given shot record are back-propagated simultaneously. The running time is linear with the number of shots, number of CPSO particles, and iterations. In our examples of 2D crosshole acquisition, the total runtime on 20 CPUs was approximately 6 h.

SYNTHETIC DATA EXAMPLE

We illustrate application of the proposed approach using a synthetic acoustic example. Acquisition layout, velocity model, and

modeled data are shown in Figure 2. The relatively complex model was parameterized as a 7×4 point bi-cubic spline interpolation, yielding nonhyperbolic first-arrival moveouts and a certain ringing effect due to energy being trapped in a low-velocity zone. In addition, despite the same source being used in all shots, there are significant amplitude differences in the recorded signal.

In Figure 3, we demonstrate the TR focusing concept using a single modeled shot record, in this case, shot #5 (see Figure 2). It is time-reversed and back-propagated using different velocity models. For the true model, at positive onset times, i.e., before reaching the true source onset time, the energy is out of focus. When this onset is reached, the energy is focused and its maximum is at the true source spatial location. If we continue back propagation to negative times, i.e., after reaching the true onset time, energy defocuses again, in a mirrored symmetry of the positive onset time behavior. Because the data have a limited bandwidth content and receiver coverage is not optimal, the spatial resolution of the focusing suffers — the source is focused to a region rather than a point. When a wrong velocity is used (either 90% or 110% of the true model), the point of maximal focusing occurs at the wrong location and onset time, indicating an error in the velocity model.

The entire data set, i.e., 10 shot records, was subsequently used for velocity model inversion using two approaches. The first is a conventional crosshole traveltime tomography. We assume that the picking is practically perfect (error is within one time sample, or 0.625 ms). The picked traveltimes were then used with a constant velocity initial model for the tomography. As a first stage, an optimal 1D model was obtained after 10 iterations. Subsequently, this model was used for a fully tomography, which converged after 20 iterations. Raypaths were recalculated at each iteration. The same data were also used without any processing for TR-based velocity estimation. Each search spline node point of the velocity model was given wide search boundaries. In this case, the range was $800 - 2200$ m/s. In Figure 4, we display the inverted model, after 600 CPSO iterations. It is compared with the traveltime tomography result and the true model. As can be clearly seen, the models are barely distinguishable from one another, and both inverted models are within 2.5% average error of the true model. In Figure 5, we show TR focusing obtained along the well using those velocity models. The TR and tomography focusing demonstrate a time-consistent behavior, i.e., all sources are focused at the same time.

Overall, due to the resemblance between the two solutions in terms of inverted models and TR focusing, we are confident in the ability of the focusing-based inversion to yield a reliable model. Such models are obtained without applying any picking procedure to the data and using the wave equation instead of its ray approximation. To validate this conclusion, we repeated the same synthetic test under the presence of strong noise in the recorded data. Figure 6 summarizes the results. Uncorrelated random noise was added to the modeled data, with an average S/N of four. A representative shot, #5 in Figure 2, is shown after noise addition in Figure 6a. Although the signal is visible, picking first arrivals would be challenging and induce errors. The CPSO algorithm was run for the noisy data using 200 particles and 600 iterations. The first 200 iterations were used to extract an optimal 1D model, exactly as was done for the noise-free test. Convergence, which is minimization of the variation functional E, is shown in Figure 6b. After 200 iterations, it seems that the algorithm has converged to the best possible 1D model because improvement is slow in iterations #50–#200. When lateral model variations are introduced, variation quickly diminishes during iterations #200–#250. Afterward, very small improvements occur until iteration #600. It is important to note that for the 1D model estimation the only constraint is a minimal and maximal velocity, and therefore convergence is rather slow. After it has been obtained, we allow a maximal 20% change for each point and thus convergence is faster in iterations #200–#250. The TR focusing obtained using the inverted model is shown in Figure 6c. It has a perfectly coherent behavior, indicating that the velocity model is correct. In addition, all noise present in the shot records has practically vanished. This is a major advantage of the suggested method — due to the implicit summation effect, noise cancels out, whereas the coherent part of the signal perseveres. In a conventional tomography approach, in which each trace would have to be picked separately, the noise effects would be much more prominent.

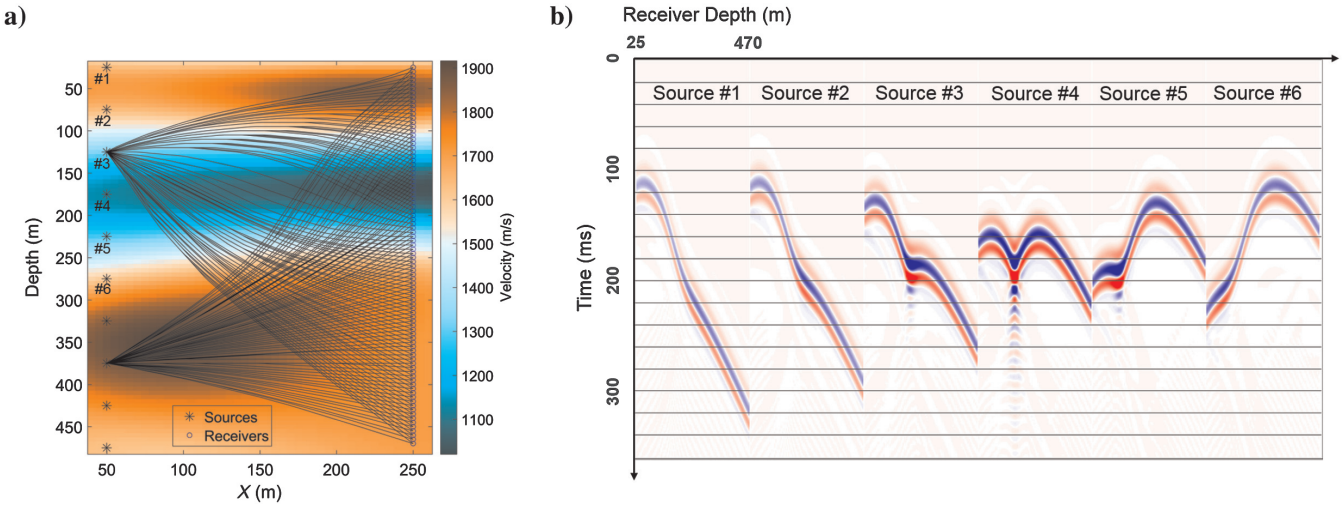

Figure 2. Synthetic crosshole example. The acquisition geometry with underlying velocity model and ray tracing for two of the source locations are shown in (a). Source locations are denoted by black asterisks and receivers by blue circles. The top six shots, modeled using acoustic finite difference, are shown in (b) with global trace normalization. Note the complex wavefronts and the amplitude differences, despite the same source being used in all shot locations. For source #4, energy is trapped within a low-velocity layer, inducing a ringing-type event.

The inverted velocity model, shown in Figure 6d, is very close to the true model and is of the same quality as the TR inverted model using noise-free data (Figure 4). Therefore, we conclude that the suggested method is also stable and robust in the presence of noise.

FIELD-DATA EXAMPLE

After demonstrating the application of the method on a synthetic example, we tested it on a dense crosshole survey. It was specifically designed for SH-wave acquisition (Lellouch and Reshef, 2017), thus yielding an effectively acoustic, albeit with an S-wave propagation velocity, data set. The survey design and representative shot records, coarsely muted around the first arrivals, are shown in Figure 7. The recorded data are quite noisy, and the first arrival wavefronts, in this case the SH-waves, have complex moveouts due to the underlying velocity field.

As a reference, the data were first manually picked and a traveltime tomography was conducted. The same data were used for the TR inversion workflow. For both cases, no a priori information except minimum and maximum velocity (200 and 800 m/s, respectively) was taken into account. For the TR model parameterization, a 5×4 bi-cubic spline interpolator was used. The two inverted models are shown in Figure 8. The differences between the models are subtle, whereas the general trend of a strong velocity gradient with depth is present in both. As discussed earlier, such small discrepancies were expected due to inherent differences between the two methods.

In Figure 9, we show focusing along the sources well obtained using the two models. It is obvious that the tomography model is inaccurate because it yields time-inconsistent focusing. The TR inverted model, however, yields a much more coherent focusing, possibly indicating its superiority.

DISCUSSION

So far, we have used the basic physical principle of TR for seismic velocity analysis. Assuming that the estimated velocity model is exact, each common-shot record that is time reversed and then back-propagated through the medium should focus at its known source location and onset time. If the constructed TR focusing along the source locations is not time consistent, i.e., different sources focus at different times, the model is necessarily erroneous. This property, combined with a wave equation and global-optimization approach, allows for a completely picking-free velocity model building in acquisitions that contain direct source-receiver paths only, e.g., VSP, RVSP, crosshole, diving waves, etc. These limitations are encountered by FWI as well, in which reflection data are challenging to incorporate.

Under practical limitations, e.g., limited aperture, finite bandwidth, low signal-to-noise, instruments response, etc., different velocity models may yield focusing of equal coherency. Nonuniqueness is an inherent part of all geophysical estimation problems (Tarantola, 2006), and finding an adequate criterion for correctness of the estimated velocity is an ever-continuing research. In this study, we opted for a focusing-based criterion, in the fashion of wave-equation migration velocity analysis techniques (Sava et al., 2005). It is possible that other criteria, e.g., extended or image domains, could have been successfully used, but our implementation is the most straightforward.

Although propagation is modeled by the full wave equation, the formulated inversion we propose is limited to measuring kinematic

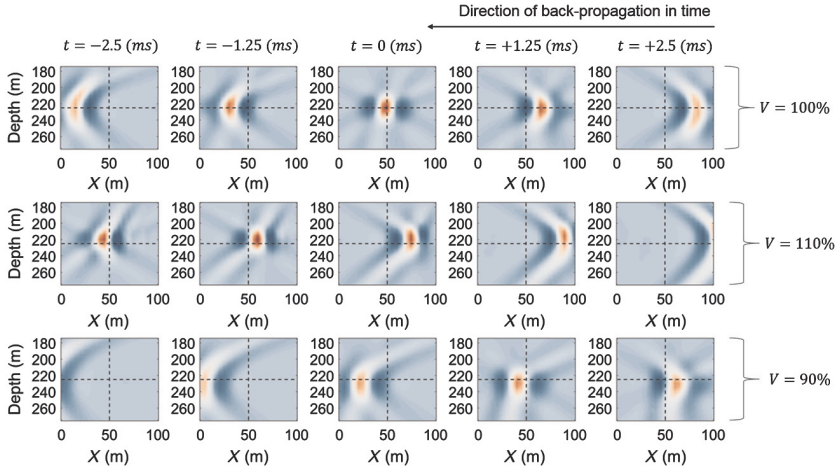

Figure 3. Focusing example of shot #5 using different velocity models. The back-propagation time advances from right to left. For the correct velocity (top row), energy is out of focus at positive times, focuses at $t = 0$ (true source onset time), and defocuses again at negative times. At $t = 0$, maximal focusing is obtained at the true source location, denoted by the intersection of the cross. For erroneous velocities (middle row: 110%, bottom row: 90%), maximal focusing occurs at a wrong location and time.

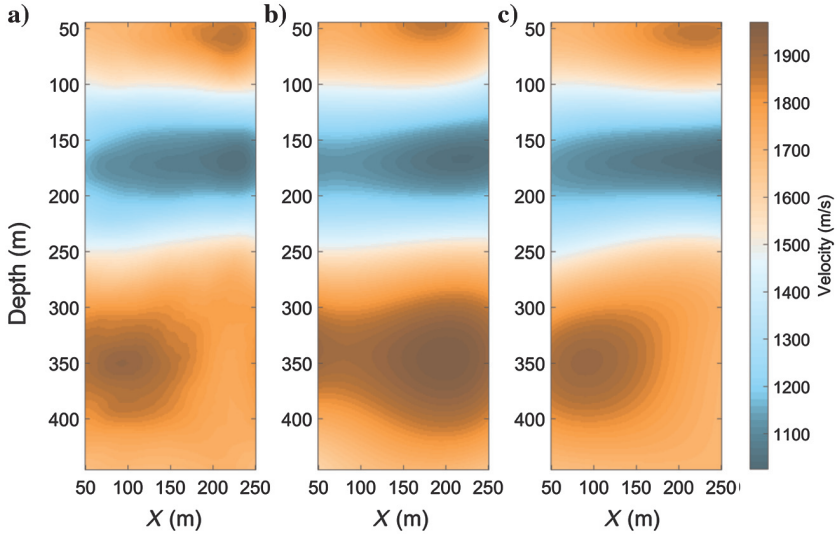

Figure 4. Inverted model comparison: the (a) tomography, (b) TR, and (c) true model are shown. The differences between the models are small, and the overall average error, computed in comparison with the true model, is less than 2.5% for both cases.

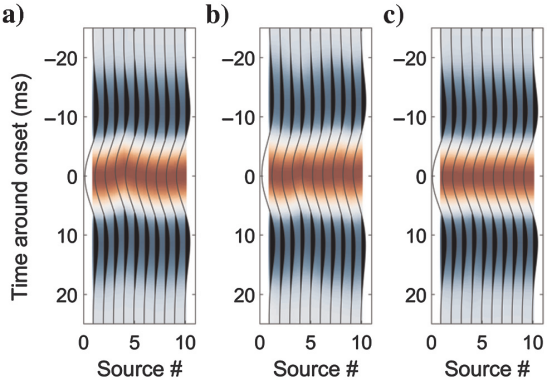

Figure 5. TR focusing using velocity models shown in Figure 4: (a) tomography, (b) TR focusing inversion, and (c) true model. Both inverted models yield time-coherent focusing, indicating their correctness.

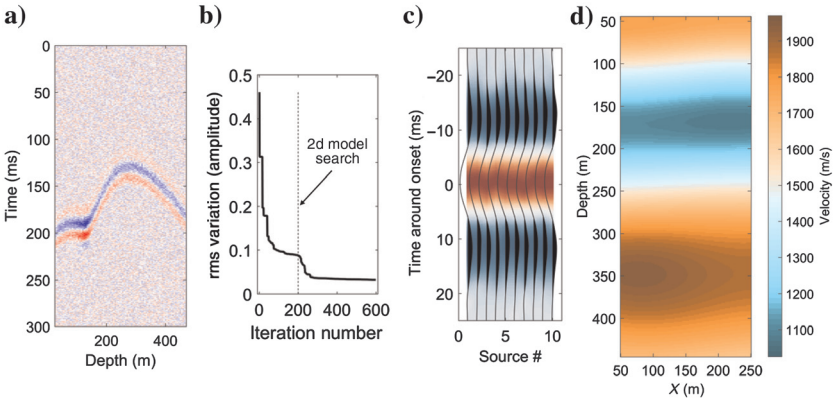

Figure 6. Sensitivity and stability of CPSO using noisy data. A representative shot record (#5 in Figure 2) with added random noise is shown in (a). Convergence of the CPSO algorithm after 600 iterations and 200 particles is shown in (b), displaying minimization of the variation functional E. For the first 200 iterations, only a 1D depth-dependent model is permitted. Afterward, lateral variations are admitted. Time focusing using the inverted model is shown in (c). Setting aside a coherent time behavior, indicating a correct velocity model, the noisiness of the input data is practically undetectable. The inverted model is shown in (d).

effects. However, TR, as a concept, allows for a correct accounting of all propagation effects (anisotropy, viscoelasticity) and true amplitude recovery. The reason we opted for the kinematic-only approach is the nonideal acquisition. In theory, assuming that the back-propagation velocity is correct, or that a physical TR experiment is conducted, the wavefield will be refocused to a spot whose dimensions are of the order of the smallest wavelength (Fink, 1997). In fact, assuming that only far-field sensing is available, focusing is limited by the classic diffraction limit. However, when the radiated wavefield is spatially improperly sampled, focusing targets will be unevenly illuminated. Such an effect is due to a combination of source/receivers geometry and the underlying velocity field. Therefore, focusing is not guaranteed to follow the diffraction limit anymore and different sources will have illumination-dependent spatial focusing patterns. In addition, different focused sources may spuriously appear to have different magnitudes, whereas such an effect is caused purely by illumination differences. One dynamic condition that may be easily introduced, even under inadequate spatial sampling, is source wavelet information. Although spatial focusing may be imperfect, its time behavior is not affected by illumination. Therefore, if the source wavelet is measured or estimated, it can be used as an objective function instead of the minimum variation E.

In comparison with a standard traveltime tomography approach, TR focusing-based inversion has several advantages. First, it does not require traveltime picking, which is time consuming and prone to errors. Second, due to the summation nature of the TR operator, incoherent noise may be canceled out during focusing. Traveltime picking, on the contrary, has to be conducted before any type of summation, i.e., on single-trace data, which is much more prone to noise. Finally, TR uses the wave equation, a more accurate representation of the propagating waves. It also allows for handling nonsmooth models, a major limitation of ray-based methods. In this study, for fairness of comparison with the tomographic approach, the models were smooth. Nonetheless, in

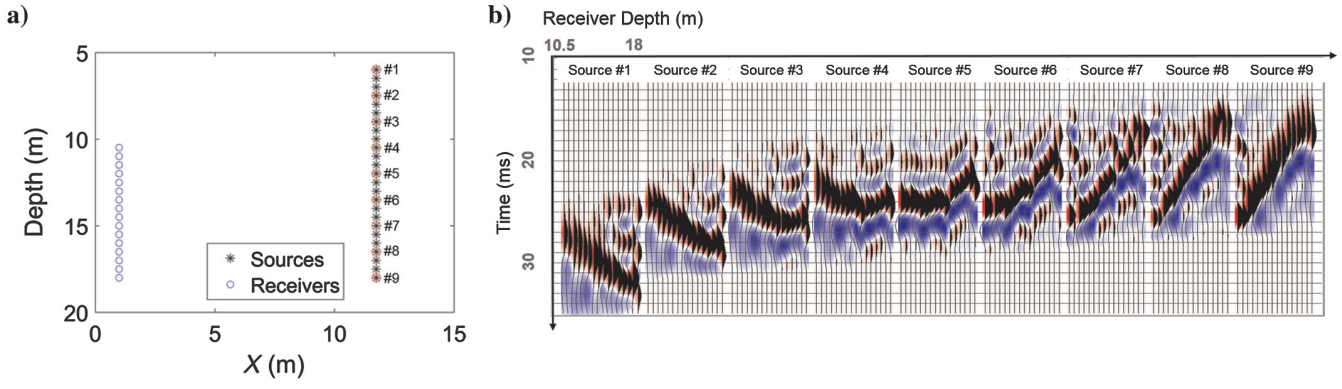

Figure 7. (a) Field crosshole acquisition setup. Source locations are denoted by the black asterisks and receivers by the blue circles. The sources displayed in (b) are marked by a red circle. They were coarsely muted around the first arrival. Because the conducted survey was using SH-waves, data may be adequately treated using an acoustic approximation. Note the complex first-arrival moveouts as well as the noisiness of the records.

more realistic, discontinuous models, the advantage of TR-based inversion would have been even clearer. A wave-equation formulation also has the ability, assuming an accurate model representation, to correctly focus multiscattered energy, most notably multiples.

The TR method aims at focusing registered energy to its origin by simultaneous back propagation of all recorded traces of the same source at its original location. An alternative approach would be conducting TR for each recorded trace separately, subsequently estimating coherency between all back-propagated traces at the known source location. Naturally, it is possible to extend this coherency to back-propagated traces at different locations as well, an assumption made in this study. Although such an alternative approach avoids the loss of receiver-dependent focusing information, it has two significant drawbacks. First, measuring coherency between single traces is very sensitive to noise, whereas integration over receivers significantly improves the S/N at the price of information loss. Second, the computational cost would be magnified by, roughly, the number of receivers. For the examples in this study, run times, given our computational means, would make the method impractical.

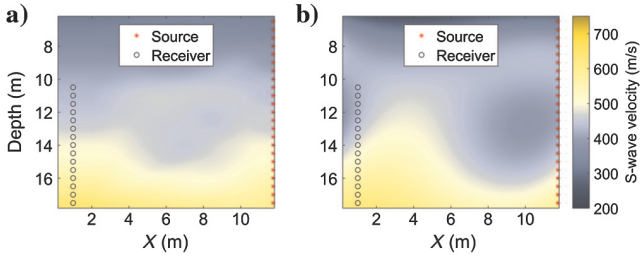

Figure 8. Inverted models obtained from (a) tomography and (b) TR focusing inversion. Source locations are denoted by the red asterisks and receivers by the black circle. Only the lower and upper boundaries of the velocity were used as a priori information, and for the TRM parameterization was a 5×4 bi-cubic spline interpolator. The general trend of increasing velocity with depth is present in both models, and the differences between them are small yet noticeable.

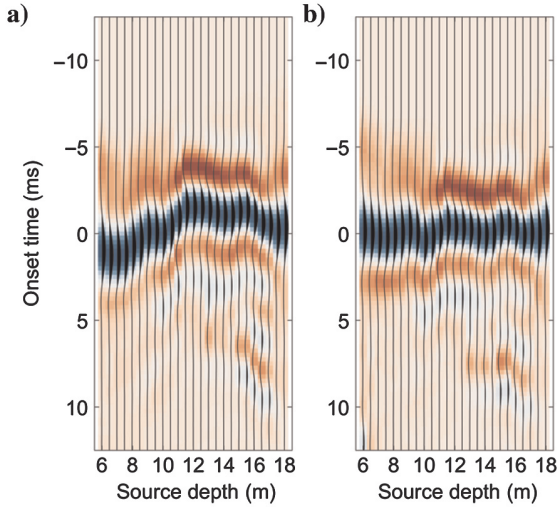

Figure 9. TR focusing along the source well, computed using the models in Figure 8. (a) Focusing obtained using the tomography model has a clearly time-inconsistent behavior, indicating an erroneous velocity model. (b) The TR model, on the contrary, yields an almost perfectly coherent focusing.

Although our wave-equation implementation is an acoustic one, it is possible to extend it to an elastic equation. In this case, focusing should occur at the same location and time for the P-wave and S-wave energy, given that the accordingly different velocity models are exact. However, assuming viscoelastic propagation, significant changes need to be made because it affects the recorded signal shape and its traveltime. Recent work by Zhu (2015) laid the foundation for such propagation in terms of the wave equation, but the underlying Q-factor field still needs to be estimated. It is possible that a joint velocity and Q TR inversion would be possible, but its complexity would be much higher.

Finally, the biggest challenge would be to generalize TR-based velocity updates for reflection data. The same principles may be applied — eventually, energy should be refocused at the source location and zero onset time. However, TR is based on emulating the physical behavior of propagating waves. Therefore, if they interact with a reflector, the propagation model should contain it. For reflection data, the velocity/density field parameterization has to allow for discontinuous models (Wapenaar and Thorbecke, 2017). In addition, as previously mentioned, multiscattered energy, especially multiples, could be used for focusing and improve its resolution. Nonetheless, an adequate velocity and density model parameterization is a major challenge.

CONCLUSION

In this study, we show a first, conceptual, implementation of the TR principle for seismic velocity analysis. It is based on the principle that given the exact velocity model the time-reversed, back-propagated recorded signal should focus at its true source location and onset time. This method has the advantage of being wave-equation based, picking-free, and solved by global optimization. It does not require any prior information on the source wavelet nor the initial velocity model.

We demonstrate its application on synthetic and field crosshole examples and compare its results with standard traveltime tomography. For the synthetic case, the model inverted using TR focusing is very close to the one obtained by tomography as well as the true model. In the field example, the focusing criterion proves the tomography model wrong. However, the TR-inverted model is relatively close to it and does not converge to a completely different solution. Therefore, we conclude the method is reliable and can be used to accurately and effectively estimate velocity models in acquisitions where direct source-receiver paths are present.

Nonetheless, the suggested inversion formulation is conceptual and relatively simplistic because it is limited to the acoustic wave equation and does not account for true source amplitude recovery as an objective function. In addition, the method in its current state can only handle direct source-receiver paths. The general case of reflections, to which the same principles may be applied, requires a different approach. TR aims at reversing the true physical propagation that waves undergo. Therefore, if they encounter a reflector in the subsurface, it should be present in the model as well. Ideally, the velocity and density should reflect that discontinuity. As an added benefit, multiscattered energy, especially multiples, would be incorporated in focusing and improve its resolution. Although

nonsmooth velocity and density model parameterizations are outside the scope of this paper, they remain a major challenge.

ACKNOWLEDGMENTS

We thank TAU's Shallow Section Research Center for the field test planning and acquisition. In addition, we thank P. Sinitsyn for traveltime picking and tomography and M. Shustak for useful discussions about focusing measures and general comments. We would also like to thank R. Dafni, I. Jones, V. C. F. Barbosa, C. Torres-Verdin, and two anonymous reviewers for their thorough reading of the manuscript and their insightful comments.

REFERENCES

Anderson, B. E., M. Griffa, P. A. Johnson, C. Larmat, and T. J. Ulrich, 2008, Time reversal: Acoustics Today, **4**, 5–16, doi: 10.1121/1.2961165.

Baysal, E., D. D. Kosloff, and J. W. C. Sherwood, 1983, Reverse time migration: Geophysics, **48**, 1514–1524, doi: 10.1190/1.1441434.

Bazargani, F., and R. Snieder, 2016, Optimal source imaging in elastic media: Geophysical Journal International, **204**, 1134–1147, doi: 10.1093/gji/ggv494.

Blomgren, P., G. Papanicolaou, and H. Zhao, 2002, Super-resolution in time-reversal acoustics: Journal of the Acoustical Society of America, **111**, 230–248, doi: 10.1121/1.1421342.

Borcea, L., G. Papanicolaou, and C. Tsogka, 2006, Coherent interferometric imaging in clutter: Geophysics, **71**, no. 4, SI165–SI175, doi: 10.1190/1.2209541.

Cao, W., S. M. Hanafy, G. T. Schuster, G. Zhan, and C. Boonyasiriwat, 2012, High-resolution and super stacking of time-reversal mirrors in locating seismic sources: Geophysical Prospecting, **60**, 1–17, doi: 10.1111/j.1365-2478.2011.00957.x.

Cassereau, D., and M. Fink, 1993, Focusing with plane time-reversal mirrors: An efficient alternative to closed cavities: Journal of the Acoustical Society of America, **94**, 2373–2386, doi: 10.1121/1.407457.

Cassereau, D., F. Wu, and M. Fink, 1990, Limits of self focusing using closed time reversal cavities and mirrors: Theory and experiment: IEEE Ultrasonics Symposium, 1613–1618.

Díaz, E., and P. Sava, 2016, Understanding the reverse time migration backscattering: Noise or signal?: Geophysical Prospecting, **64**, 581–594, doi: 10.1111/1365-2478.12232.

Fink, M., 1992, Time reversal of ultrasonic fields. I: Basic principles: IEEE Transactions on Ultrasonics, Ferroelectrics and Frequency Control, **39**, 555–566, doi: 10.1109/58.156174.

Fink, M., 1997, Time-reversed acoustics: Physics Today, **50**, 34–40, doi: 10.1063/1.881692.

Fink, M., 1999, Time-reversed acoustics: Scientific American (International Edition), **281**, 91–113.

Fink, M., 2006, Time-reversal acoustics in complex environments: Geophysics, **71**, no. 4, SI151–SI164, doi: 10.1190/1.2215356.

Guitton, A., B. Kaelin, and B. Biondi, 2007, Least-squares attenuation of reverse-time-migration artifacts: Geophysics, **72**, no. 1, S19–S23, doi: 10.1190/1.2399367.

Huang, G., R. Nammour, and W. Symes, 2017, Full-waveform inversion via source-receiver extension: Geophysics, **82**, no. 3, R153–R171, doi: 10.1190/geo2016-0301.1.

Landa, E., and A. Lellouch, 2017, Velocity model estimation using time-reversal focusing: 79th Annual International Conference and Exhibition, EAGE, Extended Abstracts, doi: 10.3997/2214-4609.201700602.

Lellouch, A., and E. Landa, 2017, Time reversal focusing for velocity estimation: Cross-well acquisition: 87th Annual International Meeting, SEG, Expanded Abstracts, 5620–5624.

Lellouch, A., and M. Reshef, 2017, Shallow diffraction imaging in an SH-wave crosshole configuration: Geophysics, **82**, no. 1, S9–S18, doi: 10.1190/geo2016-0154.1.

Luu, K., M. Noble, and A. Gesret, 2016, A competitive particle swarm optimization for nonlinear first arrival traveltime tomography: 86th Annual International Meeting, SEG, Expanded Abstracts, 2740–2744.

Poli, R., J. Kennedy, and T. Blackwell, 2007, Particle swarm optimization: Swarm Intelligence, **1**, 33–57, doi: 10.1007/s11721-007-0002-0.

Rose, J., 2002, Time reversal, focusing and exact inverse scattering, *in* M. Fink, W. A. Kuperman, J. P. Montagner, and A. Tourin, eds., Imaging of complex media with acoustic and seismic waves: Springer, 97–106.

Sava, P. C., B. Biondi, and J. Etgen, 2005, Wave-equation migration velocity analysis by focusing diffractions and reflections: Geophysics, **70**, no. 3, U19–U27, doi: 10.1190/1.1925749.

Schuster, G. T., S. Hanafy, and Y. Huang, 2012, Theory and feasibility tests for a seismic scanning tunnelling macroscope: Geophysical Journal International, **190**, 1593–1606, doi: 10.1111/j.1365-246X.2012.05564.x.

Shustak, M., and E. Landa, 2017, Time reversal diffractor detector: 87th Annual International Meeting, SEG, Expanded Abstracts, 969–973.

Tarantola, A., 2006, Popper, Bayes, and the inverse problem: Nature Physics, **2**, 492–494, doi: 10.1038/nphys375.

Van Manen, D. J., A. Curtis, and J. O. A. Robertsson, 2006, Interferometric modeling of wave propagation in inhomogeneous elastic media using time reversal and reciprocity: Geophysics, **71**, no. 4, S147–S160, doi: 10.1190/1.2213218.

Virieux, J., and S. Operto, 2009, An overview of full-waveform inversion in exploration geophysics: Geophysics, **74**, no. 6, WCC1–WCC26, doi: 10.1190/1.3238367.

Wapenaar, K., and J. Thorbecke, 2017, Virtual sources and their responses. Part I: Time-reversal acoustics and seismic interferometry: Geophysical Prospecting, **65**, 1411–1429, doi: 10.1111/1365-2478.12496.

Witten, B., and J. Shragge, 2017, Image-domain velocity inversion and event location for microseismic monitoring: Geophysics, **82**, no. 5, KS71–KS83, doi: 10.1190/geo2016-0561.1.

Zhu, T., 2015, Viscoelastic time-reversal imaging: Geophysics, **80**, no. 2, A45–A50, doi: 10.1190/geo2014-0327.1.